PERGAMON

Vision Research 39 (1999) 1759–1766

Vision Research

# Analysis of pharmacologically isolated components of the ERG

Claudia Gargini [a,b], Gian Carlo Demontis [a], Luigi Cervetto [a,b], Silvia Bisti [b,c,*]

[a] *Dipartimento di Psichiatria, Neurobiologia, Farmacologia e Biotecnologie, Universita' di Pisa, Pisa, Italy*
[b] *Istituto di Neurofisiologia del CNR, Via S. Zeno 51, 56126, Pisa, Italy*
[c] *Dipartimento Scienze e Tecnologie Biomediche STB, Università di L'Aquila, L'Aquila, Italy*

Received 27 June 1997; received in revised form 18 June 1998

**Abstract**

An harmonic analysis was applied to the electroretinogram (ERG) measured in intact cat eyes in control conditions and after pharmacological isolation of the components attributed to photoreceptors (PIII) and bipolar neurons (PII). The frequency response curves obtained in various conditions showed that the bandwidth of the PII component extends over a range of stimulus frequencies higher than the bandwidth of PIII. The enhancement of the PII response to stimuli of high temporal frequency suggests the presence of a frequency dependent gain control located either pre- and/or post-synaptically in the transmission line between the phototransductive cascade and bipolar neurons. A possible role of these processes is to enhance relevant visual information whilst selectively attenuating low frequency signals originating in the transductive cascade. 

*Keywords:* Electroretinogram; b-Wave; APB; Fourier analysis; Cat retina

## 1. Introduction

Since it's discovery, over a century ago (Holmgren, 1865, reviewed by Armington, 1974) the electroretinogram (ERG) has been a valuable tool to extract information about the electrical activity of the retina in both health and disease (see Riggs, 1986; Hood & Birch, 1994). Considerable effort has been expended to separate the various components of the electroretinographic response to uniform field stimulation and to identify the retinal cells from which they originate (e.g. Granit, 1933; Kline, Ripps & Dowling, 1978; Tomita & Yanagida, 1981; Frishman & Steinberg, 1989; Hood & Birch 1990, 1993; Breton, Schueller & Lamb, 1994). Recently there has been a renewed interest in both the functional and clinical significance of the ERG and important aspects of its cellular origin have been elucidated. There is now good evidence that the early negative-going rod-driven dark-adapted a-wave represents primarily the summed rod photocurrent which in turn reflects the kinetics of the phototransductive cascade (Hood & Birch, 1990; Lamb & Pugh, 1992; Breton et al., 1994). In addition, the analysis of pharmacologically isolated components of the ERG has indicated that the response kinetics of bipolar neurons is mirrored in the isolated PII component (Gurevich & Slaughter, 1993; Robson & Frishman, 1995). The functional dissection of the summed retinal response has also been approached by using periodic temporal modulation of both uniform field stimuli and of spatially structured stimuli of various complexity (pattern ERG) (Hess, Baker, Zrenner & Schwarzer, 1986; Baker, Hess, Olsen & Zrenner, 1988). Although this is still matter of debate (see Baker & Hess, 1984; Ringo, van Dijk & Spekreijse, 1984), the present evidence supports the notion that the first harmonic of the uniform field ERG originates from the distal layers of the retina, while the pattern ERG is generated by the elements located more proximally (Maffei & Fiorentini, 1981; Arden, Vaegan & Hogg, 1982; Maffei, Fiorentini, Bisti & Hollander, 1985). In this study we have attempted an analysis of the dynamic properties of the ERG elicited by a large uniform field whose luminance was varied sinusoidally over a range of temporal frequencies. An harmonic analysis was applied to the ERG measured from intact cat eyes in normal conditions and after pharmacological isolation of the components attributed to photore-

* Corresponding author. Tel.: +39-50-559708; fax: +39-50-559725; e-mail: silvia@neuro.in.pi.cnr.it.

0042-6989/99/$ - see front matter 
PII: S0042-6989(98)00281-8

ceptors and bipolar cells. The results provide a description of the filtering properties of the main components of the ERG and suggest that along the transmission line between photoreceptors and bipolar cells there are mechanisms for enhancing relevant temporal aspects of visual information. The value of the present approach to the generation and analysis of the ERG is in the possibility of inferring from relatively simple measurements the role of the various retinal elements in the dynamics of the visual response. A further and more specific account of the value of this analysis on the temporal properties of the ERG response is given in the following paper (Gargini, Demontis, Bisti & Cervetto, 1998, this issue).

## 2. Methods

### 2.1. Animal preparation

The data presented in this and in the following paper (Gargini et al., 1998, this issue) were obtained from experiments carried out on 33 adult cats. The measurement reported in this paper were taken from 16 animals. The experiments were carried out in accordance with the European Communities Council Directive of 24 November 1986 (86/609/EC) regarding the care and the use of animals for experimental procedures. Adequate measures were taken to minimize pain and discomfort. Anaesthesia was induced by an intramuscular injection of ketamine (Ketalar, Parke–Davis, 30 mg $Kg^{-1}$). An endotracheal tube and a venous cannula were then inserted. The animal was paralyzed with an i.v. infusion of a 0.2% solution of pancuronium bromide (Pavulon, N.V. Organon) at a rate of 0.1–0.2 ml $Kg^{-1}$ $h^{-1}$ and artificially ventilated. Anaesthesia was maintained throughout the experimental session by 3.5 mg $Kg^{-1}$ $h^{-1}$ i.v. infusion of sodium thiopental (Farmitalia). Measuraments taken during Ketamine anaesthesia, prior to thiopental infusion showed that thiopental slighty reduces the ERG amplitude. Electrocardiogram, $P_{CO_2}$ (maintained at 4–4.2%) and body temperature (maintained at 38°C) were continuously monitored. Pupils were dilated with 0.5% atropine sulfate and contact lenses with artificial pupils of 3 mm in diameter were applied. The refractive state of the eye was determined by retinoscopy and corrected with appropriate spectacle lenses. The position of papilla and area centralis were determined at the beginning of the experiment and checked again periodically using a technique described by Fernald and Chase (1971).

### 2.2. Drugs

DL-2-Amino-4-phosphonobutyrate (APB) (Calbiochem) either alone or in combination with 6-cyano-7-nitroquinoxaline-2,3 dione (CNQX) (Research Biochemicals International) and NM-DL-Aspartate (Sigma) were injected with a 27-gauge needle through the sclera into the vitreal cavity. Injection volumes were 20–100 μl and the concentration of the drugs in the vitreous was estimated assuming an average eye volume of 2.3 ml, a value obtained by direct measurements in seven animals. In three experiments $Ba^{2+}$ was also injected in the vitreal cavity (20 μl of 0.1 M solution $BaCl_2$, estimated vitreal concentration: 0.87 mM).

### 2.3. Stimuli and recording

The stimuli, recording and analyzing techniques were essentially similar to those described in a previous study (Porciatti, Burr, Morrone & Fiorentini, 1992). Two temporal patterns of luminance change were used: repeated step changes and sinusoidal changes at various temporal frequencies and modulation depth. The luminance of sinusoidal stimuli is expressed as $f(t) = L(1 + m \sin \omega t)$ where $L$ is the mean luminance and $m$ the contrast. Temporal patterns were generated by framestore (Cambridge Research VSG) and displayed on the face of a color monitor (Barco CDCT 6551, frame rate 120 Hz), by modulating the green gun. The peak spectral response for the green phosphor was at 531 nm (CIE co-ordinates: $x = 0.28$, $y = 0.605$). The visible screen was 34 cm wide and 27 cm high, subtending a visual angle of $34 \times 27°$ when viewed from 57 cm. The maximum mean luminance was 18 c $deg^{-1}$ $m^{-2}$ and could be varied by inserting neutral density filters on the light path. The retinal illumination at the maximum mean luminance level with an artificial pupil aperture of 3 mm in diameter corresponded to 221 human scotopic trolands. The ERG was recorded differentially by means of corneal silver ring electrodes from the two eyes, one of which was kept patched. Signals were amplified ($\times 20\,000$), band-pass filtered (1–100 Hz, 12 db $oct^{-1}$), digitized at 5 kHz and fed to a PC computer. Data obtained with sinusoidally modulated stimuli were then corrected to allow for the filter properties. Responses to the lowest temporal frequencies were considered only when the signal to noise ratio was above 10. In a few instances (specified in the Fig. legend) signals were dc amplified and low-pass filtered. The computer averaged the signals in synchrony with the stimulus luminance periodicity and performed a discrete Fourier analysis to estimate amplitude and phase of both fundamental and second harmonics. Amplitude and phase were also calculated separately for partial sums of the total average (20 sum packets), from which the standard error of amplitude and phase estimates were derived (see Porciatti et al., 1992). The program also averaged the signals asynchronously at 1.1 times the temporal frequency of the stimulus to give an estimate of the background noise.

## 3. Isolation of individual ERG components

The ERG is a composite response whose single components (PIII, PII and STR) add independently at the electrode. In this and in the accompaning paper (Gargini, Demontis, Bisti & Cervetto, 1999) the flash response of the principal components was isolated by the method described by Robson and Frishman (1995). The frequency characteristics of the individual components were obtained assuming that the recorded signal is the sum of contributions from parallel processes. Accordingly, the frequency characteristics of PII were isolated by vectorial subtraction of the characteristics of the pharmacologically isolated PIII from those of the ERG after suppression of STR by NM-DL-Aspartate.

## 4. Results

Averaged ERG responses to sinusoidally modulated luminance of different temporal frequency are illustrated in Fig. 1. In this example, the mean luminance (18 c $deg^{-1}$ $m^{-2}$) was modulated sinusoidally ($m =$ 84.5%) at four different temporal frequencies. The polar plots at the right hand side of each record show the signal to noise ratio of the measuraments and the dependence of the phase of the fundamental, obtained by Fourier analysis, from the frequency of the stimulus. The distortion which is seen to affect the low frequency responses more severely, is caused mainly by a prominent second harmonic component.

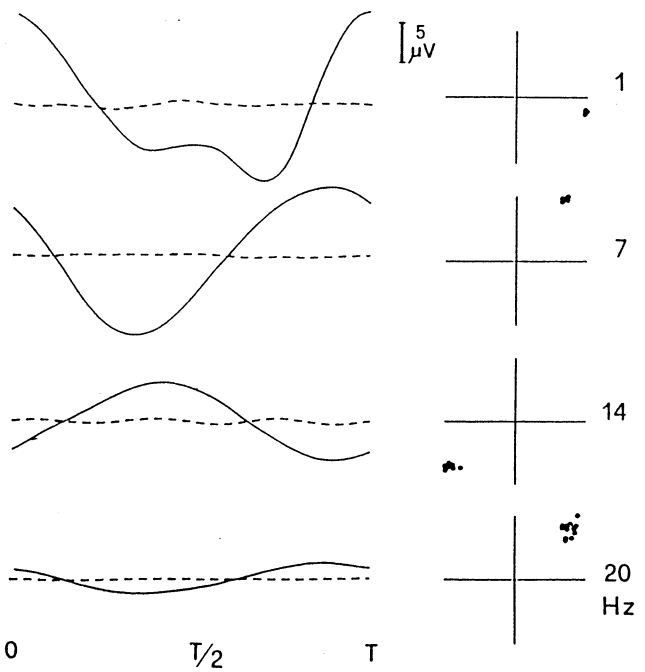


Fig. 1. Steady-state ERG in response to uniform field luminance (18 c $deg^{-1}$ $m^{-2}$) sinusoidally modulated in time ($m = 84.5\%$). Figures next to each record indicate the temporal frequency of the stimulus. Abscissa is given in units of stimulus period. Dashed traces are asynchronous noise, obtained by averaging ERG activity at a temporal frequency slightly higher than the stimulus frequency. The polar plots on the right show amplitude (norm) and phase (argument) of the first harmonic modulation of partial averages of 10–20 individual 20-sum packets. The two-dimensional scatter of this plot gives an estimate of variance of the amplitude and phase, reported as error bars in the following curves. Note that the scale amplitude in the polar plots is normalized.

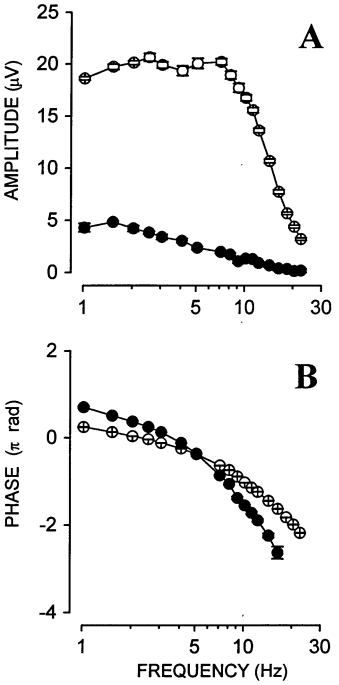


Fig. 2. (A) Response amplitude of the first (open circles) and second (filled circles) harmonic as a function of the temporal frequency of the sinusoidally modulated luminance ($L = 18$ c $deg^{-1}$ $m^{-2}$, $m = 84.5\%$). (B) The corresponding phase of responses in A as a function of the temporal frequency.

The attenuation and phase characteristics of both fundamental and second harmonic components constructed by plotting the response amplitude and the phase as a function of the temporal frequency of the stimulus are plotted in Fig. 2. The attenuation characteristics of the fundamental showed considerable variability with the state of adaptation and between animals. Also the contribution of the second harmonic was variable, and depended mainly on the frequency and modulation depth of the stimuli. At 1 Hz and with $m = 84.5\%$, the amplitude of the second harmonic typically was about 20% of the total response.

Fig. 3 illustrates the results of an experiment in which the usual tests of linearity were applied. The traces in A show the stimulus protocol which consisted of four sequences of sinusoidal modulation of the same mean luminance at four different contrasts ($m = 7.9, 20.1, 41$ and 84.5%); the corresponding attenuation characteristics of the fundamental are reported in B. The dotted lines superimposed on responses at different contrasts

were constructed by fitting the frequency response characteristics at the lowest contrast and multiplying by the appropriate proportionality factor. It is seen that superposition holds up fairly well to modulation contrasts of about 50% while a significant deviation from linearity can be appreciated for modulation depths of 84.5%. The phase characteristics illustrated in C appear largely independent of the contrast.

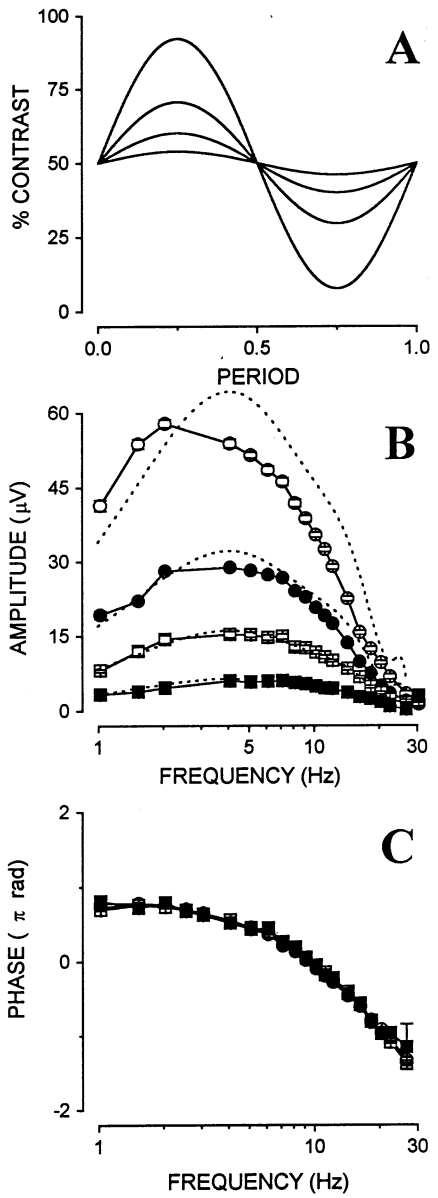


Fig. 3. (A) Reconstruction over a single period of the stimulus consisting of a mean luminance of 18 c $deg^{-1}$ $m^{-2}$ sinusoidally modulated at four contrasts ($m = 7.9, 20.1, 41, 84.5\%$). (B and C) attenuation and phase characteristics of the first harmonic component (fundamental) obtained with the stimuli reported in A ($m = 7.9\%$, filled squares; 20.1%, open squares; 41% filled circles; 84.5% open circles). Dashed lines in B were obtained by fitting the frequency response data to the lowest stimulus contrast and multiplying by the appropriate proportionality factor.

All the above observations support the notion that the uniform field ERG response is non-linear and that a linear behavior can be approximated when the stimulus contrast is maintained within a range not exceeding a 50% modulation.

The attenuation characteristics shown in Fig. 3 are similar to those which would be imposed on a non-attenuated signal by a band-pass filter with a bandwidth of about 1–10 Hz. Attenuation and phase characteristics of the ERG response were also seen to depend on the level of adapting light. In general the response amplitude approximately doubled for each tenfold increase in luminance and the phase lag decreased as the mean luminance increased. The dependence of the attenuation and phase characteristics on the mean luminance is related to the well known effect of the adapting level on both amplitude and kinetics of the light response. It is well known that attenuating light from an external source delays vision. This however may also be due to a transition from the cone to rod pathway.

The mass ERG current recorded with external electrodes is the sum of many components generated by a large number of electrically active cell types and by the Mueller cell response to local changes in $K^+$ concentration (see Newman & Odette, 1984). For all practical purposes it can be reasonably presumed that photoreceptors contribute to the complex ERG response with the initial phase of the negative going PIII component, bipolar neurons with the positive going PII and proximal retinal neurons such as amacrine and or ganglion cells with the negative-going scotopic threshold response (STR) (Frishman & Steinberg, 1989). A pharmacological dissection of the summed ERG currents has been in fact obtained by selectively blocking synaptic transmission with intravitreal injections of glutamate agonists and antagonists (Robson & Frishman, 1995). In the cat retina the photoreceptor component can be isolated by blocking synaptic transmission to second order neurons with APB (Slaughter & Miller, 1981), whereas the STR can be removed by blocking NMDA receptors present on inner retinal neurons (Vaegan & Millar, 1994).

The effects of intravitreal injections of NM-DL-A were first explored. This agent has been found especially effective in suppressing inner retinal responses in the cat (Robson & Frishman, 1995). Application of NM-DL-A caused an increase of the b-wave amplitude and a marked change in the attenuation characteristics. Averaged responses from three separate experiments are reported in Fig. 4 where attenuation and phase characteristics of the fundamental in responses in control (open circles) and NM-DL-A (filled circles) are compared. Open diamonds in Fig. 4 were obtained by vector subtraction of amplitude and phase of the fundamental in NM-DL-A from control. The main effect of NM-DL-A was to increase the response amplitude in the frequency range of 1–8 Hz thus sharpening the

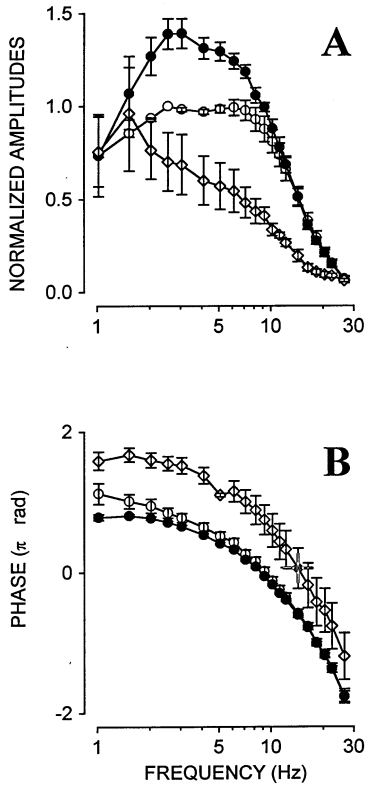


Fig. 4. (A) Attenuation characteristics of the fundamental, obtained by averaging responses from three separate experiments. Open circles: control conditions; filled circles: after intraocular injection of NM-DL-A (estimated local concentration: 2 mM). Diamonds: vector difference of post-NM-DL-A responses from control responses. Data are normalized to the control response at 1 Hz. (B) Phase characteristics of data in A. Vertical bars are the S.E. of the average. Mean luminance 18 c $deg^{-1}$ $m^{-2}$.

bandpass character of the filtering. Assuming that NM-DL-A abolishes completely the STR signal, the subtraction data should describe the temporal properties of the inner retina elements responsible for its generation. However, given the adaptation level used in the present study, the removal of the inner retina signals might also be due to generators other than those in the dark circuit that generate STR.

In an attempt to isolate other ERG components, the receptor agonist APB was injected into eyes previously treated with NM-DL-A. The results are illustrated in Fig. 5. The trace in A indicates the step change in luminance used as a stimulus; records in B and C are the responses obtained in NM-DL-A and APB, respectively, the trace in D was computed subtracting B from C. If one assumes the APB isolated component to be the mass current generated in photoreceptors, then, the waveform in D should represent the summed light response of the ON bipolar neurons, which in cat are believed to be the principal contributors to the PII component of the full field ERG (see: Robson & Frishman, 1995).

In three experiments the injection of APB was associated with that of the receptor antagonist CNQX which is expected to block selectively the response of OFF bipolar neurons (Robson & Frishman, 1995). The results of these measures showed no difference compared with those in APB alone. This finding offers further support to the notion that the contribution of the OFF bipolar neurons to the cat ERG is negligible. In order to explore the extent of the Mueller cell contribution to the various ERG components, the inward rectifying $K^+$ channels were blocked by combining other treatments with intravitreal injections of $Ba^{2+}$ (Newman, 1993). In these conditions the ERG and its components as well were indistinguishable from those obtained in the absence of the $Ba^{2+}$-block.

The frequency characteristics of the isolated PII (mainly ON bipolar neurons) were obtained by vector subtraction of amplitude and phase of the fundamental after APB and NM-DL-A from amplitude and phase in control. Fig. 6(A) reports the attenuation characteristics of the fundamental after APB block (filled circles)

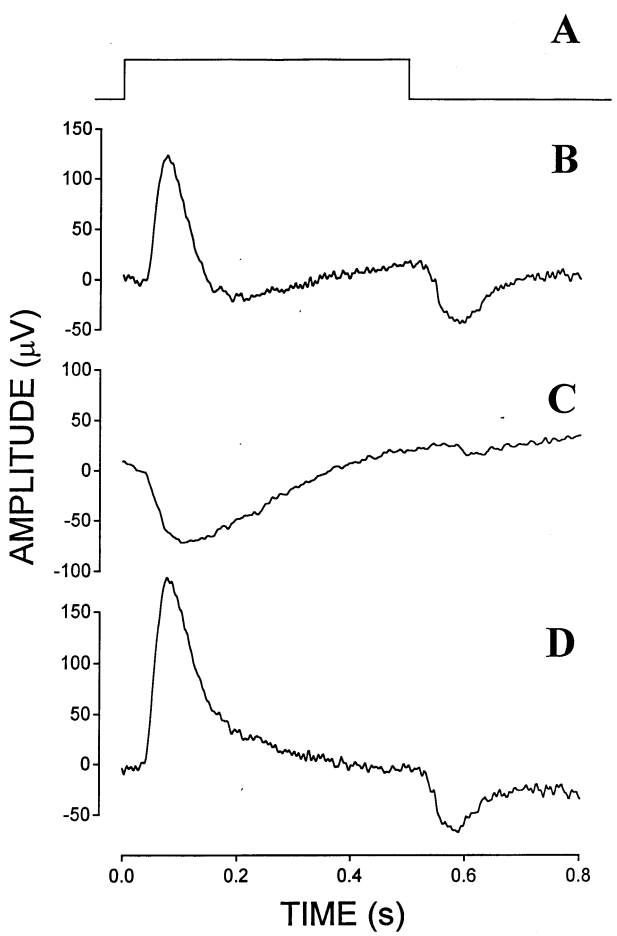


Fig. 5. DC recordings of the ERG to a stepped luminance (2.85–34 c $deg^{-1}$ $m^{-2}$), (A) time course of the light stimulus (B) response in NM-DL-A, (C) after injection of APB (estimated local concentration: 2 mM), (D) computed difference (B–C).

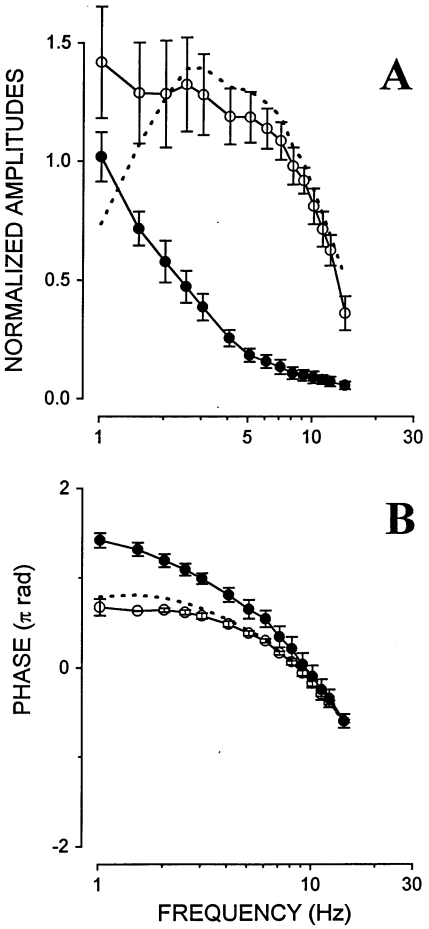


Fig. 6. (A) Attenuation characteristics of the APB isolated PIII component (filled circles). Open circles: responses derived by vector subtraction of the post-APB records from the post-NM-DL-A records in Fig. 4. The dashed curve is the best fit of the post-NM-DL-A data of Fig. 4. (B) Phase characteristics of responses in A. Mean luminance 18 c $deg^{-1}$ $m^{-2}$.

as the average of three measurements. The characteristics in control and NM-DL-A (dashed line) are the same as shown in Fig. 4. The computed PII component (open circles), which we assume to be generated by ON bipolar neurons is marked by the open circles. The corresponding phase characteristics are illustrated in B. Considering that the fundamental accounts for by over 90% of the total response, data in Fig. 6 should approximate the Fourier trasform of the responses illustrated in Fig. 5(C and D). The response bandwidth of bipolar neurons is much wider than that of the isolated PIII with an almost tenfold difference in the cut-off frequency. A striking feature of this difference is that in the range between 5 and 10 Hz the photoreceptor component becomes vanishingly small while bipolar neurons are still responding near maximally. This may suggest that the transfer of signals from photoreceptors to bipolar neurons is subjected to a differentiation process whereby the slowest signals contained in the receptor response are attenuated. This feature may serve to extract relevant visual information from signals contaminated by low frequency noise of photoreceptor origin (Baylor & Fettiplace, 1977).

Although the present analysis was conducted on the fundamental component of the frequency response, it must be noted that the harmonic analysis of the isolated PIII and PII also showed that, in addition to a dominating fundamental, a significant second harmonic is always present at high luminance contrasts, particularly at the lowest stimulus frequencies. The amplitude and phase characteristics of the second harmonic in different conditions and for isolated ERG components are reported in Fig. 7. A shows the attenuation characteristics of the second harmonic component in control ERG (open circles), in NM-DL-A (filled circles) and in APB (squares). B shows the corresponding phases of A. In APB a significant second harmonic (10% of the fundamental) could be measured at 1 Hz (filled circles). These results show that generators of the second harmonic response are also present in the earliest stages of retinal processing (see Baker et al., 1988).

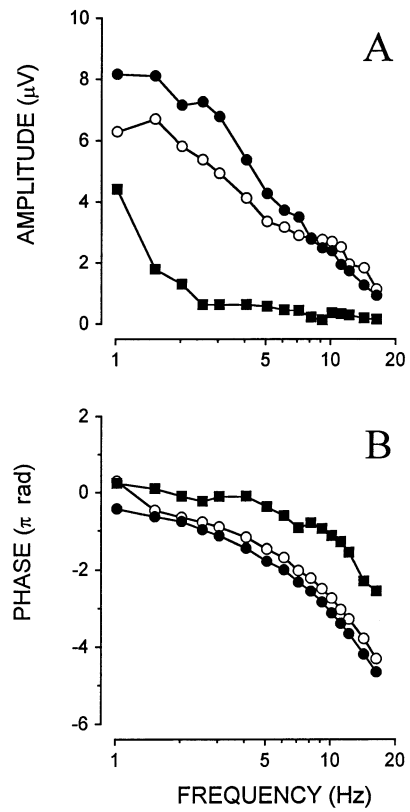


Fig. 7. (A) Attenuation characteristics of the second harmonic component in control ERG (open circles), after NM-DL-A (filled circles), after APB (squares). (B) Phase characteristics of data in A.

## 5. Discussion

When considering the cellular origin of the various components recorded in the different experimental conditions described in the present study, it seems reasonable to assume that the normal ERG results mainly from a combination of currents generated by photoreceptors and ON- bipolar neurons, with possible contributions originating from Mueller cells (Dick & Miller, 1985). It must be emphasized, however, that, although of photoreceptor origin, the early PIII does not reflect the input to the bipolar neurons. The available evidence (Hood & Birch, 1990; Breton et al., 1994) indicates that the early component of the a-wave reflects the kinetics of the cGMP cascade in photoreceptors.

The temporal properties of the retinal elements that generate the ERG response can be analyzed separately by combining a pharmacological approach with the harmonic analysis of the response to periodic stimuli. Attenuation and phase characteristics of the fundamental satisfy linearity up to modulation depths of 50%. Responses to low frequency sinusoidal stimuli at high luminance contrasts of ERG and of isolated PIII and PII components exhibit a substantial second harmonic distortion.

Comparison of the attenuation and phase characteristics of normal ERG with the characteristics of the isolated PIII and PII components reveals different filtering properties: band-pass like for normal ERG and low-pass for the APB-isolated PIII. The characteristics of the PII component obtained by subtraction suggest that in the transfer of signals to bipolar neurons a boosting of the gain in the frequency range of 5–10 Hz enhances the response to high frequencies producing a considerable extension of the response bandwidth.

In their extensive analysis in the turtle retina Baylor and Fettiplace (1977) suggested that the synaptic transfer from photoreceptors to ganglion cells occurs over a cascade of delay and differentiating stages whose kinetics seem to be matched to extract temporally relevant visual signals whilst attenuating noise present in the slow signals near the input. In the present study, we show that filtering and differentiating mechanisms of appropriate kinetics are present between photoreceptors and bipolar neurons. The processes responsible for these transformations may be located presynaptically and due to the filtering properties of the inner segment membrane of photoreceptors. Alternatively they may reflect either synaptic or post-synaptic events. The voltage changes that modulate transmitter release at the synaptic contacts with bipolar neurons are shaped by the voltage dependent conductance of the inner segment membrane. Therefore the evaluation of the kinetics of the PII component requires the knowledge of the properties of the actual input to bipolar neurons, that is the voltage response of photoreceptors. The role played by the photovoltage in determining the frequency response of the ERG components is analyzed in the companion paper that reports ERGs in conditions that modify the kinetics of the voltage response in photoreceptors (Gargini et al., 1999).

## Acknowledgements

The authors would like to thank Dr Concetta Morrone and Professor David C. Burr for valuable discussions and critical reading of the manuscript, Mr Giulio Cesare Cappagli for patient and helpful technical assistance and Mrs Danila Moriconi for animal care. C.G. was supported by Dr Karl Thomae GmbH. This work was supported in part by MURST 60% to S.B. and MURST 40% to L.C.

## References

Arden, G. B., Vaegan, & Hogg, C. R. (1982). Clinical experimental evidence that the pattern electroretinogram (PERG) is generated in more proximal retinal layers than the focal electroretinogram (FERG). *Annual NY Academy of Sciences*, *388*, 580–601.

Armington, J. C. (1974). *The Electroretinogram*. New York: Academic Press.

Baker, C. L. Jr., & Hess, R. F. (1984). Linear and nonlinear components of human electroretinogram. *Journal of Neurophysiology*, *51*, 952–967.

Baker, C. L. Jr., Hess, R. F., Olsen, B. T., & Zrenner, E. (1988). Current source density analysis of linear and non-linear components in the primate electroretinogram. *Journal of Physiology*, *407*, 155–176.

Baylor, D. A., & Fettiplace, R. (1977). Kinetics of synaptic transfer from photoreceptors to ganglion cells in turtle retina. *Journal of Physiology*, *271*, 425–448.

Breton, M. E., Schueller, A. W., & Lamb, T. D. (1994). Analysis of ERG a-wave amplification and kinetics in terms of the G-protein cascade of phototransduction. *Investigative Ophthalmology & Visual Sciences*, *35*, 295–309.

Dick, E., & Miller, R. F. (1985). Extracellular $K^+$ activity changes related to electroretinogram components. *Journal of General Physiology*, *85*, 911–931.

Fernald, R., & Chase, R. (1971). An improved method for plotting retinal landmarks and focusing the eyes. *Vision Research*, *11*, 95–96.

Frishman, L. J., & Steinberg, R. H. (1989). Light evoked increases of $K^+$ proximal portion of dark-adapted cat retina. *Journal of Neurophysiology*, *61*, 1223–1243.

Gargini, C., Demontis, G. C., Bisti, S., & Cervetto, L. (1999). The effect of blocking the rod hyperpolarization activated current ($I_h$) on the cat electroretinogram. *Vision Research*, *39*, 1767–1774.

Granit, R. (1933). The components of the retinal action potential in mammals and their relation to discharge of optic nerve. *Journal of Physiology*, *77*, 207–240.

Gurevich, L., & Slaughter, M. M. (1993). Comparison of the waveforms of the ON bipolar neuron and the b-wave of the electroretinogram. *Vision Research*, *33*, 2431–2435.

Hess, R. F., Baker, C. L., Zrenner, E., & Schwarzer, J. (1986). Differences between electroretinograms of cat and primate. *Journal of Neurophysiology*, *56*, 747–768.

Holmgren, F. (1865). En method att objectivera effecten af Ijusintryck pa retina. *Upsala Lakareforenings Forhandlingar*, *1*, 177–191.

Hood, D. C., & Birch, D. G. (1990). A quantitative measure of the electrical activity of human rod photoreceptors using electroretinography. *Visual Neuroscience*, *5*, 379–387.

Hood, D. C., & Birch, D. G. (1993). Light adaptation of human rod receptors: leading edge of human a-wave and models of rod receptor activity. *Vision Research*, *33*, 1605–1618.

Hood, D. C., & Birch, D. G. (1994). Rod phototransduction in retinitis pigmentosa: estimation and interpretation of parameters derived from the rod a-wave. *Investigative Ophthalmology & Visual Sciences*, *35*, 2948–2961.

Kline, R., Ripps, M., & Dowling, J. E. (1978). Generation of b-wave currents in the skate retina. *Proceedings of the National Academy of Sciences USA*, *75*, 5727–5731.

Lamb, T. D., & Pugh, E. N. Jr. (1992). A quantitative account of the activation steps involved in phototransduction in amphibian photoreceptors. *Journal of Physiology*, *499*, 719–758.

Maffei, L., & Fiorentini, A. (1981). Electroretinographic response before and after section of the optic nerve. *Science*, *211*, 953–954.

Maffei, L., Fiorentini, A., Bisti, S., & Hollander, H. (1985). Pattern ERG in the monkey after section of the optic nerve. *Brain Research*, *59*, 423–425.

Newman, E. A. (1993). Inward-rectifying Potassium Channels in Retinal Glial (Mueller) Cells. *Journal of Neuroscience*, *13*, 3333–3345.

Newman, E. A., & Odette, L. L. (1984). Model of electroretinogram b-wave generation: A test of the $K^+$ hypothesis. *Journal of Neurophysiology*, *51*, 164–182.

Porciatti, V., Burr, D. C., Morrone, M. C., & Fiorentini, A. (1992). The effects of ageing on the pattern electroretinogram and visual evoked potential in humans. *Vision Research*, *32*, 1199–1209.

Riggs, L. A. (1986). Electroretinography. *Vision Research*, *26*, 1443–1460.

Ringo, J., van Dijk, B., & Spekreijse, H. (1984). Pattern ERG of the cat. *Vision Research*, *24*, 859–865.

Robson, J. G., & Frishman, L. J. (1995). Response linearity and kinetics of the cat retina: the bipolar cell component of the dark-adapted electroretinogram. *Visual Neuroscience*, *12*, 837–850.

Slaughter, M. M., & Miller, R. F. (1981). 2-amino-4-phosphonobutyric acid-new pharmacological tool for retina research. *Science*, *211*, 182–185.

Tomita, T., & Yanagida, T. (1981). Origins of the ERG waves. *Vision Research*, *21*, 1703–1707.

Vaegan, & Millar, T. J. (1994). Effect of Kainic Acid and NMDA on the pattern electroretinogram, the scotopic threshold response, the oscillatory potentials and the electroretinogram in the urethane anaesthetized cat. *Vision Research*, *34*, 1111–1125.